

EVALUATION OF CFRP-REFERENCE SAMPLES FOR POROSITY MADE BY DRILLING AND COMPARISON WITH INDUSTRIAL POROSITY SAMPLES BY MEANS OF QUANTITATIVE XCT.

Bernhard PLANK¹, Guruprasad RAO¹, Johann KASTNER¹

¹ University of Applied Sciences Upper Austria, Wels, Austria
bernhard.plank@fh-wels.at, Stelzhamerstraße 23, 4600 Wels, Austria

Abstract. The main objective of this work was to find a new way to create reference samples for the quantitative evaluation of porosity in carbon fibre reinforced polymers (CFRP) by means of X-ray computed tomography (XCT). Artificial porosity samples for an exact determination of porosity were made by drilling several hundred holes into CFRP laminates with a diameter between 200 to 300 μm . The diameters were evaluated by optical microscopy and XCT to obtain reference porosity values. Results show void contents between 0.96 and 4.81 vol.%.

Using these artificial porosity samples five different threshold methods were compared. An adapted method from Airbus and ISO50 threshold led to best results for the artificial porosity samples.

In addition to the reference samples two different types of industrial porosity samples were investigated. The void morphology differed between both types. Type 1 is characterized by a high amount of micro- and meso voids (> 90 %) and type 2 contained only macro voids. Varying voxel size from $(2.75 \mu\text{m})^3$ to $(120 \mu\text{m})^3$ we showed that for the type 1 sample it was more important to choose a proper threshold method than for a type 2 sample. For type 1, FHW method and for type 2 ISO50 methods led to the best results for a broad voxel size variation. Further it was shown, that at high resolution it is less critical to choose a proper threshold. In a next step, the evaluated porosity at high resolution can be used to calibrate or adapt a threshold method to obtain useful results for lower resolution (larger sample size).

Our final conclusion is that for each individual sample and material type a proper threshold method in combination with optimised XCT measurement parameters has to be chosen to obtain reliable quantitative porosity values.

1. Motivation and Introduction

The importance of carbon fibre reinforced polymers (CFRP) in the aeronautical industry is increasing from year to year. Safety-critical structures are inspected completely. A main challenge is that porosity can critically weaken material strength. For example, the interlaminar shear strength decreases by about 7 % per 1 vol. % porosity, up to a total porosity of 4 vol. % [1].

The standard non-destructive testing (NDT) method for porosity detection in CFRP is ultrasonic testing (UT). Ultrasonic velocity and attenuation measurement can be used to estimate the porosity level [1, 2]. In addition to UT active thermography (IR) is a promising NDT method for porosity and defect detection for the future [3, 4, 5, 6]. To interpret UT or

IR correctly much inspector experience is needed and in some cases an interpretation is still not possible. For this reason X-ray computed tomography (XCT) is an ideal supplementary 3D method [7, 8]. XCT is a contactless non-destructive method which can nowadays reach a high resolution down to $< 1 \mu\text{m}$. In [9] XCT was used to evaluate the mechanical properties of unidirectional CFRP with respect to evaluated porosity and pore morphology. The main drawback of XCT is that the resolution depends mainly on the sample size. Therefore for larger samples the resolution has to be reduced significantly.

To estimate porosity within CFRP samples all mentioned NDT methods have a collective drawback: there are no methods to obtain accurate porosity values as references. The most common reference standard nowadays is acid digestion that shows an uncertainty level of $\pm 1 \text{ vol. \%}$ [10]. For UT the estimated absolute deviation is in the range of around $\pm 0.5 \text{ vol. \%}$ [5, 11].

In [12] Nikishkov et al. drilled twenty 0.3 mm deep holes with a diameter of 0.1 mm using a micro-drill in a unidirectional Carbon/Epoxy specimen to evaluate the error of different threshold methods. The focus of Nikishkov et al. was the correct representation of the diameter near the surface. Different threshold methods were compared with light optical measurements. In addition, a dependence on XCT resolution was observed. No porosity evaluation was done by Nikishkov et al. on these drill holes. In our study CFRP reference plates for exact porosity were made by drilling several hundreds of holes with a diameter between 200 to 300 μm resulting in void contents between 1 and 4.5 vol. %. The diameters were evaluated by optical microscopy and by means of XCT to obtain reference porosity.

2. Experimental

2.1 Investigated CFRP Samples

In this work two types of CFRP samples with porosity were investigated: artificial porosity samples made by drilling and industrial porosity samples the from aeronautic industry.

2.1.1 Artificial Porosity Samples

For the artificial porosity samples we used plates with 5 ply of PREPREG C 970/PWC T300 3K UT (TY) in plain weave style. In the case of a non-porous material it consists of 60 wt. % carbon fibres and 40 wt. % epoxy resin. The prepreg ply thickness was 0.2159 mm. Figure 1 shows an overview of the manufactured samples (D1 to D3). Sample dimensions including mounting holes are $20 \times 60 \times 1 \text{ mm}^3$. Total area including the drill holes was $17 \times 17 \text{ mm}^2$ in the centre of the samples. Altogether 1,750 drill holes were induced in three different plates with a diameter of 0.2 and 0.3 mm.

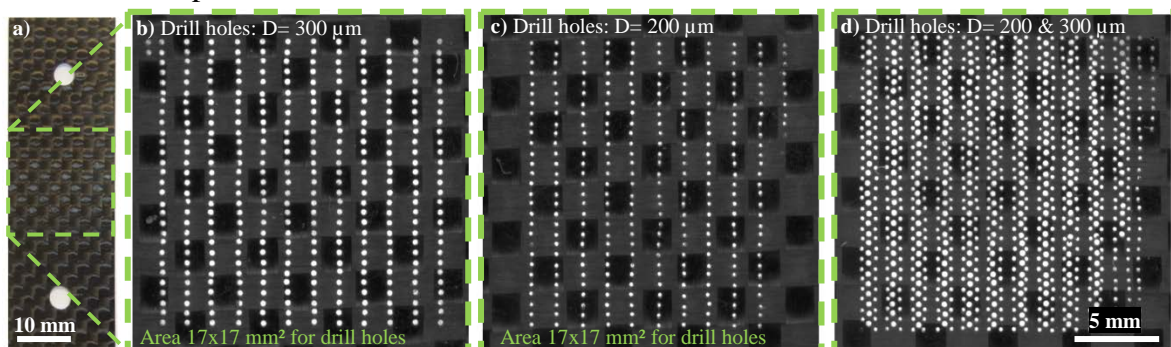


Fig. 1. (a) Overview of one undrilled plate (sample N0 - $20 \times 60 \times 1 \text{ mm}^3$) and the $17 \times 17 \text{ mm}^2$ area containing the drill holes. (b) Detail of drilled sample D2 with 350 holes at D0.3 mm, (c) drilled sample D1 with 300 holes at D0.2 mm and (d) drilled sample D3 with 700 holes at D0.2 mm and 310 holes at D0.3 mm.

To create a porosity reference sample with closed holes different combinations of the drilled plates (D1 to D3) and undrilled plates (N0) were joined. Because sample thickness the amount, and the diameter of the drill holes is known the porosity for each plate combination can be calculated. In Figure 2 XCT images of one combination with an expected porosity of 4.69 – 4.93 vol. % is shown. In this study porosity samples with a defined porosity between 0.96 and 4.81 vol. % were investigated

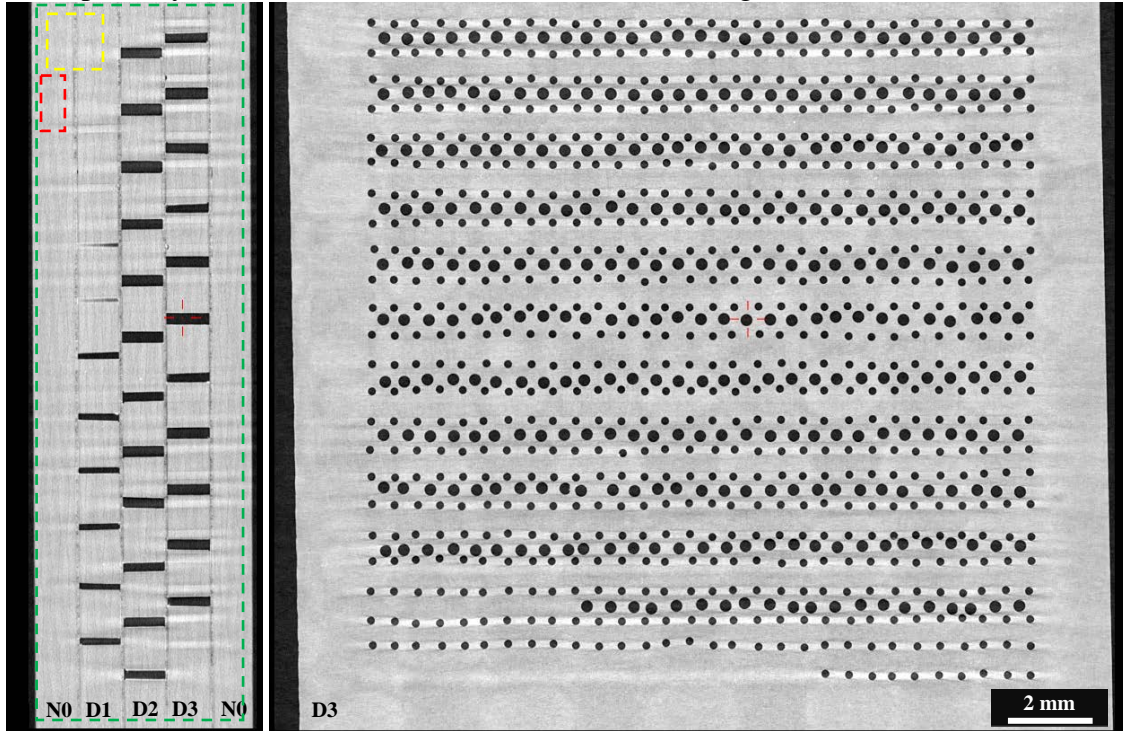


Fig. 2. XCT-slice images of a combination I of different plates (N0 - D1 - D2 - D3 - N0) to create an artificial porosity reference sample with an expected porosity of 4.69 – 4.93 vol. %. Dashed lines indicate the region of interest for calculating the thresholds: green for ISO50, OTSU and MaxD; yellow: Airbus adapted and red: Airbus. (11 μm)³.

2.1.1.1 Reference Measurements of Artificial Porosity Samples

The individual plate thickness and the thickness of each combination were measured at five different points using a screw gauge (Preisser Messtechnik, Germany). Drill hole diameters were measured by optical microscopy (LOM) at a magnification of 50x with an Olympus microscope (BX51). Each drill hole was measured from one side of the plates by using manual 3-point circle fitting in the software PicEd. In addition to microscopy, XCT scans on the centred region of the plates were performed with 5 μm voxel size for measuring the diameters by fitting a cylinder. By XCT for sample plate D1 65, for D2 65, and for D3 130 holes were evaluated.

2.1.2 Industrial Porosity Samples

To compare the results from our artificial pore structures we furthermore investigated two different types of CFRP samples with real porosity inside. One sample (type 1) was made of 20 plies PREPREG C 970/PWC T300 3K UT (TY) in plain weave style with approximately 5.0 vol. %. The second sample (type 2) was made from 16 plies of bi-diagonal (0°/90°) layers with 12k rovings and RTM6 resin with approximately 1.7 vol. % of porosity. To be able to perform voxel-size variation XCT scans with a minimum voxel size of (2.75 μm)³ cross-section area for each sample was below 5x5 mm².

2.2 X-Ray Computed Tomography

XCT scans were performed on a Nanotom 180 NF device manufactured by GE phoenix|x-ray. The device uses a 180 keV nano-focus tube and a full digital 2304^2 pixel flat panel detector (Hamamatsu). Molybdenum was used as target material. No pre- or post-filters were used for the scans. Applied voltage on the X-ray tube was 60 kV at a voxel size between $(2.75 \mu\text{m})^3$ and $(120 \mu\text{m})^3$. Voxel sizes were calibrated by a 3.9796 ± 0.0020 mm ball bar manufactured by GE.

2.3 Data Processing

XCT data processing and evaluation was done in VGStudio Max 2.2 from Volume Graphics. Thresholds were calculated in our in-house tool iAnalyse developed by the University of Applied Sciences Upper Austria. 32 to 16 bit mapping was done manually.

2.4 Applied Threshold Methods for Segmentation of Voids

Various kinds of threshold methods have been described in the literature. The primary segmentation method is based on an algorithm introduced by Otsu [13] for grey level segmentation based on histograms. Apart from OTSU threshold (Otsu) we used maximum distance threshold (MaxD) and the FH-Wels method (FW) [14, 15] as well as Airbus threshold (Airbus) [16] and ISO50 threshold (ISO50) in our analysis.

- Otsu threshold is an automatic threshold-selection method for bimodal histograms implemented in iAnalyse. The histogram is divided into two classes minimizing the intra-class variance and maximizing the inter-class variance. Thus the separability of the resulting classes in grey levels is maximized. [13]
- MaxD threshold is applied using iAnalyse by indicating the maximum distance from the line joining two histogram peaks of the air-peak and the material-peak. [14, 15]
- FW method is a combination of Otsu and MaxD threshold values. It is assumed that the correct porosity is in between these two thresholds. The exact factor has to be determined empirically by high resolution measurements for the specific CFRP sample types. For CFRP industrial porosity sample type 1, 73 % of gained Otsu and 27 % of MaxD threshold was determined. [15]
- ISO50 threshold is the mid-point grey value of the material and air peak. It can be obtained both from iAnalyse and VG Studio Max 2.2. Instead of the mid-point grey value (50 %) this method can easily adapt between 0 % (air-peak) and 100 % (material-peak) for further calibration purpose.
- Airbus threshold method is obtained as a grey level of a non-porous region of the CFRP sample found by incremental examination of volume where the percentage of material reaches 0.01 %. Therefore a non-porous reference sample or a larger region with no porosity is required for each scan (Figure 2: dashed green region). [16]
- Airbus adapted threshold is used for evaluation of our artificial porosity samples using the same principle as Airbus threshold [16] but the region of interest for evaluating the threshold was adapted and includes CFRP resin, fibre, and filler material between the air-gap (Figure 2: dashed yellow region).

3. Results and Discussion

3.1 Artificial Porosity Samples

3.1.1 Determination of Reference Porosity Values

Measurement of the diameters by light optical microscopy was not effective because there were too many breakouts and differences between the front and back sides of the plates. Finally high resolution scans at $(5 \mu\text{m})^3$ were performed and cylinders were fitted for 65 drill holes per sample plate to get a mean diameter and deviation. For comparison of the front and back side results, cylinders with only 0.2 mm in depth were evaluated for each side by XCT. In Table 1 the evaluated mean diameters are shown. Highest deviation is obvious for Plate D1 between the front and back side of the plates evaluated by LOM. Evaluation by XCT shows only small differences in the range of maximum $\pm 1.45 \mu\text{m}$ between front and back side. For final porosity estimation the diameters of the entire cylinders measured by XCT are used.

Table 1. Results of diameter evaluations drill holes of plates D1, D2 and D3. Sample size 65.

Plate	Mean Diameter LOM [μm]		Mean Diameter XCT [μm]		
	Front	Back	Front (0.2 mm)	Back (0.2 mm)	Entire cylinder
D1	183.76 \pm 10.14	167.32 \pm 13.16	193.45 \pm 1.85	192.79 \pm 2.75	192.69 \pm 0.59
D2	284.23 \pm 6.85	284.68 \pm 7.26	292.87 \pm 1.36	293.62 \pm 1.03	293.6 \pm 0.83
D3 small	189.24 \pm 9.18	184.67 \pm 7.38	195.09 \pm 1.29	196.34 \pm 0.88	196.05 \pm 0.92
D3 big	278.97 \pm 8.00	287.25 \pm 7.00	291.09 \pm 1.20	294.00 \pm 1.44	293.37 \pm 0.89

The overall deviation (δQ) for the diameters used for porosity calculation is given by

$$\delta Q = \sqrt{\delta a^2 + \delta b^2 + \delta c^2},$$

where δa , δb and δc are the standard deviations from front, back, and the entire cylinder of each plate and drill hole type. Together with the thickness of the individual plates, the mean diameter and amount of drill holes a total void volume was calculated. In combination with the total sample volume, given by the measured thickness of the chosen combination, the following expected porosity's were calculated (Table 2) for a region of interest of 17 x17 mm²:

Table 2. Expected range of porosity percentages for various combinations within a region of 17 x17 mm²

	Plates	Expected porosity range (vol. %)
Combination I	N0-D1-D2-D3-N0	4.81 \pm 0.12
Combination II	N0-D3-N0	4.56 \pm 0.08
Combination III	N0-D2-N0	2.58 \pm 0.03
Combination IV	N0-D1-N0	0.96 \pm 0.02

3.1.2 Comparison with Various Threshold Methods

In Figure 3 the results of the evaluated porosity for combination I (4.81 \pm 0.12 vol. %) and combination III (2.58 \pm 0.03 vol. %) are depicted. In dependence of the used threshold method there are big differences in the results. For combination I, Airbus adapted, ISO50, and OTSU leads to the closest results. For combination III Airbus adapted has the smallest deviation from the expected porosity.

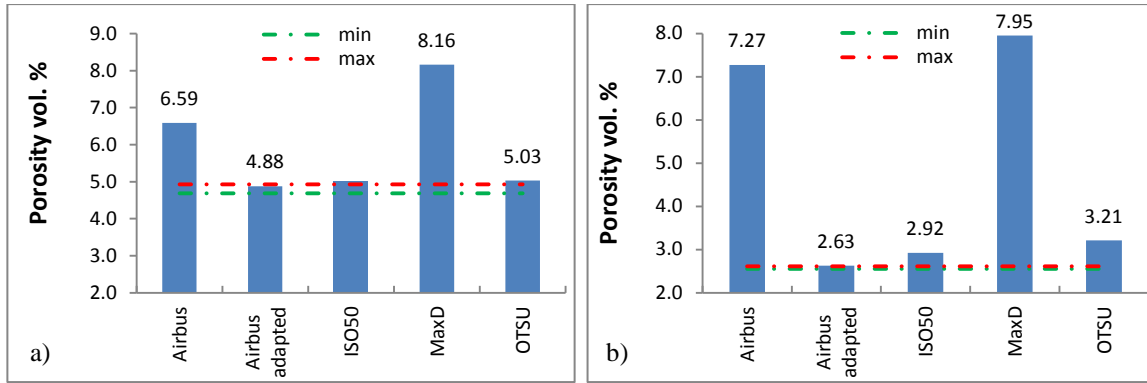


Fig. 3. Porosity for combination I (a) & III (b) at various thresholds scanned at $11 \mu\text{m}^3$ VS

Table 3 shows the deviation in vol. percentage points from the expected mean porosity for various thresholds in combination I, II, III, and IV. The applied Airbus-adapted threshold shows minimum deviation. It has to be noted that this Airbus-adapted threshold is already improved by choosing a separate region of interest containing the gap between individual plates. The published Airbus threshold method [16] needs a reference sample or region without any pores. ISO50 also delivers quite close and constant porosity values, having the advantage to be able to adjust it by using for example ISO46 instead of ISO50. OTSU threshold shows an average deviation and Airbus and MaxD thresholds show maximum deviation for all combinations. The FHW threshold method was not applied for these specimens because calibration was not possible. The necessary threshold value should lie below OTSU. The FHW method was developed for smaller pore morphology whereas the correct threshold is expected between OTSU and MaxD.

Table 3. Deviation of vol. % porosity from expected mean porosity for combination I to combination IV

Threshold	Deviation from expected mean porosity [vol. %]			
	Combination I (4.81 vol. %)	Combination II (4.56 vol. %)	Combination III (2.58 vol. %)	Combination IV (0.96 vol. %)
Airbus adapted [16]	+ 0.07	- 0.42	+ 0.05	- 0.04
ISO50	+ 0.19	+ 0.24	+ 0.34	+ 0.04
OTSU [13]	+ 0.22	+ 0.38	+ 0.63	+ 0.11
Airbus [16]	+ 1.78	+ 2.96	+ 4.69	+ 3.07
MaxD [14, 15]	+ 3.35	+ 4.06	+ 5.37	+ 4.48

* Segmentations of air gap between plates are partial present. Further optimisation is necessary.

3.2 Industrial Porosity Samples

In Figure 4 (left) XCT images with real porosity in CFRP type 1 and type 2 are shown. CFRP type 1 has a stronger X-ray absorption compared to type 2. In type 1 micro- and macro pores are visible. In CFRP type 2 only macro pores are available which are located in the neat resin areas. In type 2 these neat resin areas can be clearly distinguished from the C-fibre yarns. These differences between CFRP types are also visible in the grey value histograms (right). In the overview the material peak of type 1 looks similar to a Gaussian curve. For CFRP type 2 the whole material peak is shifted to lower grey values and in addition a clear second shoulder is visible at lower grey values due to the neat resin. In the detailed view large differences between the air (void) peak and material peaks are visible. The main reason is the different size distribution of the voids. For type 2 a simple threshold

around 27,500 seems to be feasible. For industrial porosity sample type 1 (red) the proper threshold position is not so clear because many micro-pores have a grey value between the clear air and material peak. In addition, a histogram of one artificial porosity sample (combination I) is added. In this sample the air and material peaks look similar to Gaussian curves.

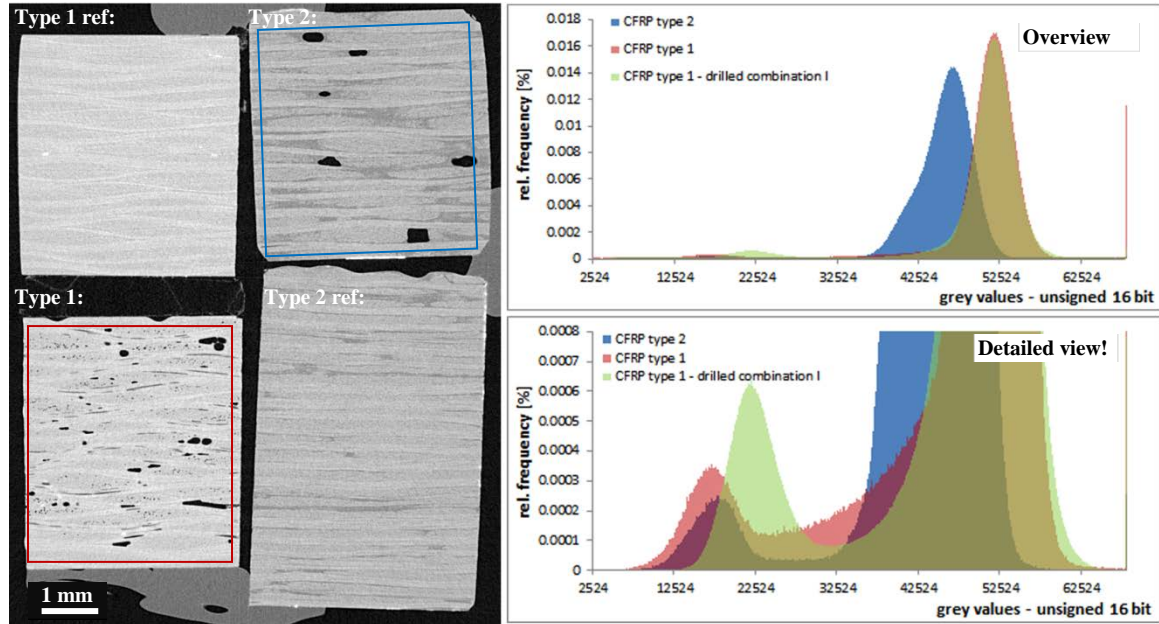


Fig. 4. CFRP samples of type 1 and type 2 with and without porosity (left). Histograms of the grey values of industrial porosity samples (right) type 1 (red), type 2 (blue), and drilled artificial porosity sample type 1 from Figure 2 (green)

To describe the different voids within a CFRP sample we classified them in five categories in decreasing order depending on the occupied volume in Table 4.

Table 4. Classes and used colour code for voids displayed in Figure 5

Ranges of volume in [μm^3]	Class	ideal sphere diameter [μm]	Void type
60×10^6 above	Class I	> 486	Joint- macro-voids
7×10^6 - 60×10^6	Class II	237-486	macro-voids
1×10^6 - 7×10^6	Class III	124-237	meso-voids
100×10^3 - 1×10^6	Class IV	58-124	meso-voids
27×10^3 - 100×10^3	Class V	37-58	micro-voids

In Figure 5 voids within CFRP type 1 and type 2 are displayed and colour coded according to Table 3. In type 2 only macro voids of class I (red), class II (green), and a low amount of meso-voids of class III (pink) are present. In CFRP type 1 all 5 classes of voids are present including many micro-voids of class V (yellow). Comparing the total number for type 1 of segmented voids approximately 45 % of the voids are classified to class V and another 45 % to class IV. Influence of these two classes on total porosity is less than 30 % (Class V 4 %; Class IV 24 %).

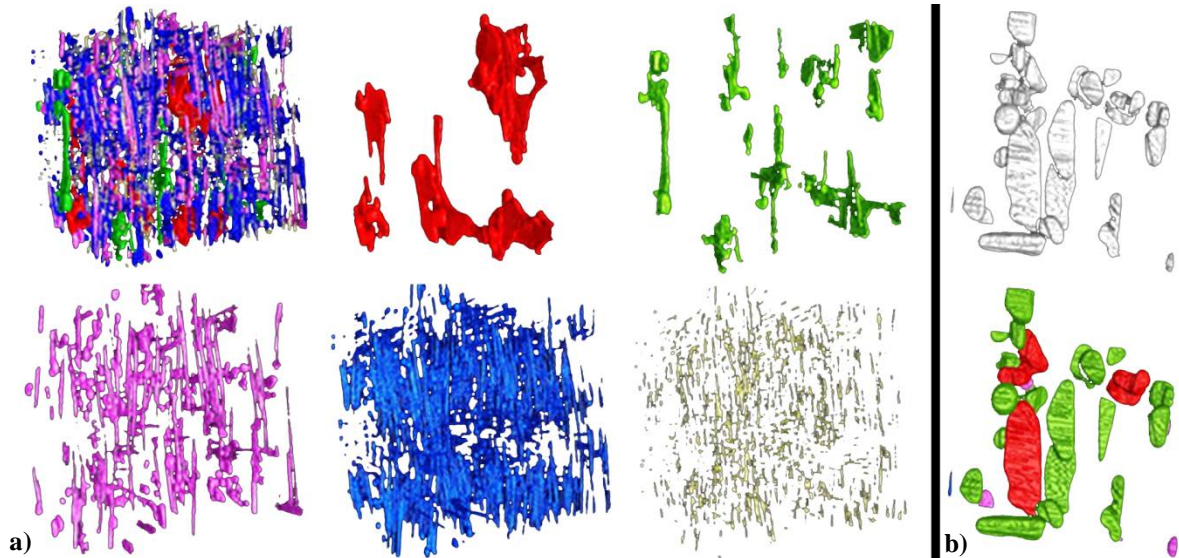


Fig. 5. CFRP samples of type 1 (a) and type 2 (b) with real porosity. Voids are colour coded according to the respective volume classes I (red), II (green), III (pink), IV (blue), and V (yellow) introduced in Table 3. Samples scanned at $7.5 \mu\text{m}^3$ VS and segmented with ISO50 threshold. Field of view: $3.21 \times 10^9 \mu\text{m}^3$.

3.2.1 Voxel Size Variation Scans and Porosity Evaluation with Various Threshold Methods

To evaluate how different threshold methods act at different resolutions voxel variation scans between $(2.75 \mu\text{m})^3$ and $(120 \mu\text{m})^3$ were performed on the industrial porosity samples CFRP type 1 and type 2. In addition, voxel size variation scans could be used to find a correct porosity within a specimen because at high resolution the exact threshold method is not as important compared to lower resolutions. For CFRP type 1 in Figure 6 it is clearly visible that on high resolution scans ($< (5 \mu\text{m})^3$ voxel size), all applied threshold methods resulting in a rather similar result. As soon as the resolution decreases the results of different thresholding methods vary significantly. For CFRP type 1 FHW threshold which was developed and calibrated for this material system [13, 14] the porosity is quite constant at approximately ± 1 vol. % till $(60 \mu\text{m})^3$ VS.

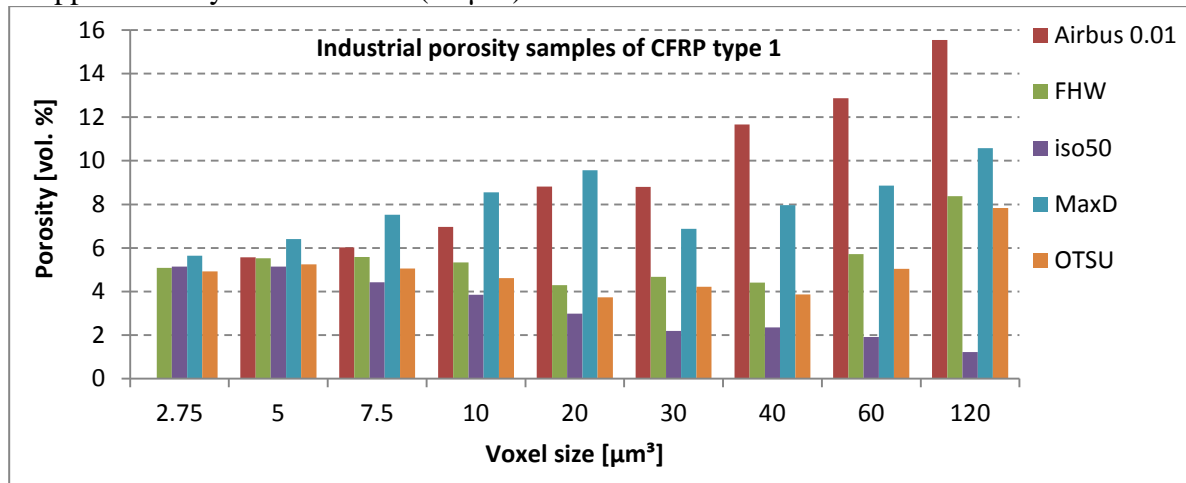


Fig. 6. Voxel size variation scans: porosity evaluated at various thresholds - industrial porosity sample type 1

For CFRP type 2 in Figure 7 there are some abnormalities with the high resolution scans at $(2.75 \mu\text{m})^3$. The reason for that is mainly a wrongly calculated OTSU threshold. Due to the high resolution the material peak in the histogram has two clear shoulders, one peak for epoxy resin and another for the C-fibres. This leads to a wrong threshold calculation for OTSU and in a further step also for FHW method. Above $(5 \mu\text{m})^3$ voxel size

all applied threshold methods gives nearly the same porosity results till approximately $(20 \mu\text{m})^3$. This small variation between the threshold methods results from the relatively large macro-voids within the sample compared to CFRP type 1. Above $(20 \mu\text{m})^3$ ISO50 threshold leads to the most constant porosity values for this individual sample and material type.

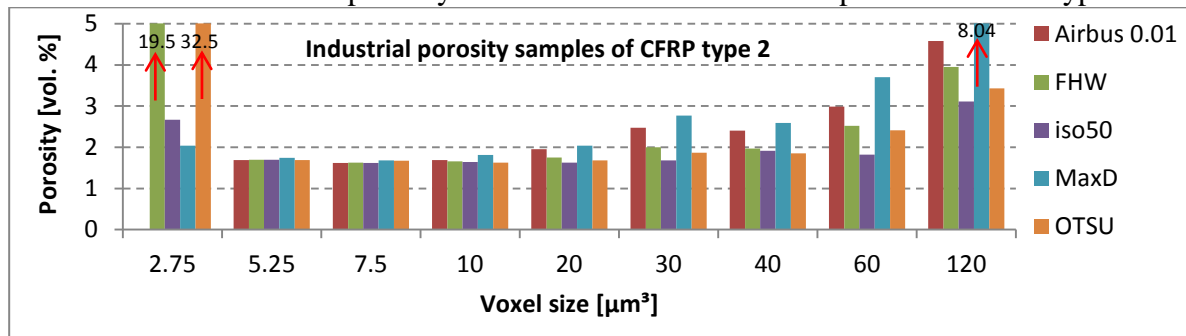


Fig. 7. Voxel size variation scans: porosity evaluated at various thresholds - industrial porosity sample type 2

For artificial porosity samples a similar trend as in the industrial porosity sample of CFRP type 2 is expected. That is mainly due to the fact that in both samples only bigger macro-voids and drill holes classified to Class I and II are present.

4. Conclusion and Outlook

In this study we introduced a new way to create reference samples for a quantitative porosity evaluation by means of X-ray computed tomography. Due to the relatively large drill holes with a diameter of 200 and 300 μm only macro-voids could be artificially created. In future experiments smaller voids should also be created. An additional drawback of these artificial porosity samples is the air-gap between individual plates. This air gap can be closed quite well by filler material so that it is more or less invisible in XCT. But some additional segmentations of the air gap are still present in the results so optimisations are necessary in further investigations, as depicted in Figure 8. Especially if higher thresholds are applied segmentation of this filler-material increases disproportionately as visible for MaxD and Airbus results. For other NDT methods such as UT or IR these samples will not work due to the gaps between the individual plates.

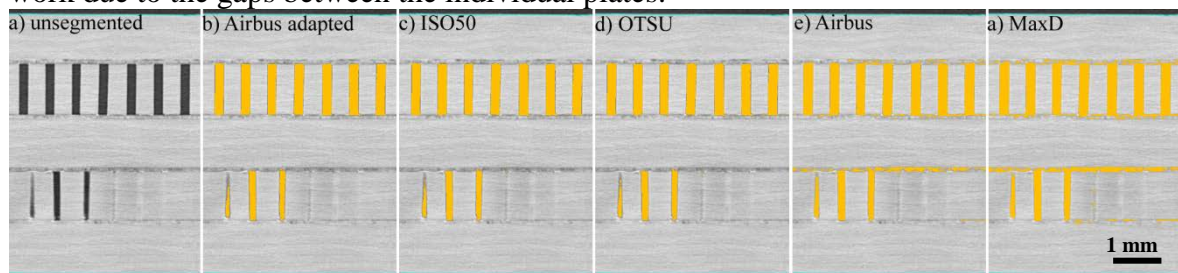


Fig. 8. Segmentation of induced porosity sample combination I with various threshold methods. $(11 \mu\text{m})^3$ VS

In order to create a meaningful amount of drill holes which directly correlate with porosity, until now it was only possible to create diameters not smaller than 200 μm in 1 mm thick CFRP. That means that the volume of the individually induced pores is comparable with the investigated industrial porosity samples of CFRP type 2. For a comparison of CFRP type 1 still smaller drill holes are necessary.

The voxel size variation scans and porosity evaluation with various threshold methods showed that this is a good way to obtain information about an unknown material. At a high resolution it is less critical to choose a proper threshold. In a further step the evaluated porosity with the lowest deviation between different threshold methods could be used to calibrate or adapt a method to obtain useful results for lower resolution (larger

sample size). After that kind of calibration simple methods such as ISO “x” may lead to good results for specified measurement parameters and similar void morphology.

Acknowledgment

The authors would like to thank J. Šekelja from FACC AG and D. Kiefel and R. Stoessel from AIRBUS for manufacturing the specimens. We would also like to thank R. Zemann from TU Vienna for doing parameter studies to drill small holes and Peter Orgill and Sascha Senck for proofreading. The work was financed by the K-Project ZPT+, supported by the COMET programme of FFG and by the federal government of Upper Austria and Styria.

References

- [1] E.A. Birt, R.A. Smith, A review of NDE methods for porosity measurement in fibre-reinforced polymer composites, *Insight*, 46 (11) (2004), pp. 681–686.
- [2] D.E.W. Stone, B. Clarke, Ultrasonic attenuation as a measure of void content in carbon-fibre reinforced plastics, *Non-destr Test*, 8 (1975), pp. 137–145.
- [3] M.P. Connolly, The measurement of porosity in composite materials using infrared thermography, *J Reinf Plast Compos*, 2 (1992), pp. 1367–1375.
- [4] D.M. Heath, W.P. Winfree, Thermal diffusivity measurement in carbon-carbon composites, D.O. Thompson, D.E. Chimenti (Eds.), *Proceedings of the review of quantitative nondestructive evaluation*, vol. 88 Plenum Press, New York (1989), pp. 1613–1619.
- [5] G. Mayr, B. Plank, J. Sekelja, G. Hendorfer, Active thermography as a quantitative method for non-destructive evaluation of porous carbon fiber reinforced polymers, *NDT & E International*, Volume 44, Issue 7, November 2011, pp. 537–543.
- [6] G. Mayr, B. Plank, J. Gruber, J. Sekelja, G. Hendorfer - Thermal diffusivity measurements of porous CFRP specimens with different number of plies using pulsed thermography in transmission and reflection mode - *Proceedings of 12th Quantitative InfraRed Thermography Conference*, Bordeaux, France, 2014, pp. 10.
- [7] B. Plank, F. Ellert, J. Gruber, C. Gusenbauer, J. Kastner - Detektion von Fehlern in kohlenstofffaserverstärkten Kunststoffen mittels Sichtprüfung, Ultraschallprüfung, Radioskopie, aktiver Thermografie und Röntgen Computertomografie. - *DGZfP Jahrestagung 2013*, Dresden, Germany, 2013, pp. 9.
- [8] B. Plank, G. Mayr, A. Reh, D. Kiefel, R. Stössel, J. Kastner, Evaluation and Visualisation of Shape Factors in Dependence of the Void Content within CFRP by Means of X-ray Computed Tomography - *Proceedings of 11th European Conference on Non-Destructive Testing (ECNDT 2014)*, Prague, Czech Republic, 2014, pp. 9.
- [9] A. Stamopoulos, K. Tserpes, P. Prucha and D. Vavrik, Evaluation of porosity effects on the mechanical properties of carbon fiber-reinforced plastic unidirectional laminates by X-ray computed tomography and mechanical testing, *Journal of Composite Materials* 0(0), pp. 12.
- [10] ISO 14127. Carbon-fibre-reinforced composites-determination of the resin, fibre and void contents, 1st ed., 2008.
- [11] L. Lin, M. Luo, H. T. Tian, X. M. Li, G. P. Guo, Experimental investigation on porosity of carbon fiber-reinforced composite using ultrasonic attenuation coefficient, *17th World Conference on Nondestructive Testing*, 25-28 Oct 2008, Shanghai, China.
- [12] Y. Nikishkov, L. Aioldi, A. Makeev, Measurement of voids in composites by X-ray Computed Tomography, *Composites Science and Technology* 89 (2013), pp. 89–97.
- [13] Otsu, N., 1975. A threshold selection method from gray-level histograms. *Automatica*, 11(285-296), pp. 23-27.
- [14] B. Plank, J. Sekelja, G. Mayr, J. Kastner - Porositätsbestimmung in der Flugzeugindustrie mittels Röntgen-Computertomografie - *Proceedings Industrielle Computertomografie Fachtagung 2010*, Wels, Austria, 2010, pp. 25-34.
- [15] J. Kastner, B. Plank, D. Salaberger, J. Sekelja - Defect and porosity determination of fibre reinforced polymers by x-ray Computed Tomography - *2nd Int. Symposium on NDT in Aerospace*, Hamburg, Germany, 2010, pp. 12.
- [16] R. Stoessel, D. Kiefel, R. Oster, B. Diewel, L. Llopart Prieto, μ -Computed Tomography for 3D Porosity Evaluation in Carbon Fiber Reinforced Plastics (CFRP), *International Symposium on Digi-tal Industrial Radiology and Computed Tomography*, 2011, pp. 7.